Regularities of mechanical behavior of steel 40Cr during the postcritical deformation of specimens in condition of necking effect at tension

M.P. Tretyakov*, T.V. Tretyakova, V.E. Wildemann
Center of Experimental Mechanics, Perm National Research Polytechnic University, Komsomolskiy Ave. 29, 614990, Perm, Russia
cem_tretyakov@mail.ru, http://orcid.org/0000-0001-6146-6769
cem.tretyakova@gmail.com, http://orcid.org/0000-0001-9445-5185
wildemann@pstu.ru, http://orcid.org/0000-0002-6240-4022

ABSTRACT. The work is devoted to the experimental study of mechanical behavior regularities of the structural steel 40Cr under postcritical deformation of specimens in conditions of strain localization formation in the form of neck during extension. The results of testing specimens cut from the initial samples with a neck are given. Various levels of preliminary postcritical deformation of initial samples are implemented. Using a noncontact 3D video system for recording displacement and strain fields of Vic 3D Correlated Solutions, based on the digital images correlation technique, the displacement and strain fields in the gauge length of both the original specimens with the neck and after the groove were recorded in two different schemes to eliminate geometrical heterogeneity. On the base of obtained results, the stiffness and strength of 40Cr steel were evaluated in a necked specimen at various stages of postcritical deformation. It is shown that the material in the peripheral areas of the gauge length of the sample is in a strengthened state, which does not depend on the degree of previously achieved postcritical deformation, and the strength of the material in the neck-forming zone on the initial specimens is thereby increased.

KEYWORDS. Experimental mechanics, postcritical deformation, strain localization, neck, tension, digital image correlation.

Citation: Tretyakov, M.P., Tretyakova, T.V., Wildemann, V.E., Regularities of mechanical behavior of steel 40Cr during the postcritical deformation of specimens in condition of necking effect at tension, Frattura ed Integrità Strutturale, 43 (2018) 146-154.

Received: 01.11.2017
Accepted: 05.11.2017
Published: 01.01.2018

INTRODUCTION

Currently, the attention of a large number of researchers is aimed at studying various aspects of deformation processes, accumulation of damages and destruction of structural materials. This is due to the ever-increasing demands on load-bearing capacity, reliability and safety of critical structural elements with simultaneous tightening

of requirements for their material consumption. In the context of approach development devoted to the forecasting the construction element destruction, which requires solving such problems like structural integrity on the base of deformation process and material destruction modeling processes. One should take into account the mechanical behavior of materials at the postcritical stage, characterized in the experiment by a load decrease with increasing elongation and immediately precedes the moment of sample failure. The necessity and relevance of the fundamental study of various aspects of material behavior at the postcritical stage of deformation is mentioned in papers [1-6].

The material deformation at the postcritical stage of deformation is accompanied by actively proceeding plasticity processes and in most cases leads to the localization of strain as a necking effect in the gauge length of the specimen. This effect in the test significantly complicates the registration, processing and interpretation of the experimental data [7-10]. However, obtaining experimental data in the localization conditions in the form of a neck is of scientific and practical interest in order to understand the processes characterizing the plastic and postcritical deformation and destruction of structural materials, the theoretical description and modeling of the material behavior in structures, and process simulation [11-15].

In the following sources [2, 4, 15] the basis of mathematical theory of stable postcritical deformation processes of softening media is developed. In [16-19], methodological issues of testing were considered and experimental data of postcritical behavior of structural steels and alloys under various types of stress-strain state and temperatures were obtained. A comparison of the criteria for the proceeding of the deformation process to the postcritical stage under various types of stress-strain state was made [20]. Analytical and numerical solutions of boundary value problems, performing carrying capacity reserves and the increase of the survivability of structures and bodies with cracks considering the postcritical deformation of materials are obtained [21-23].

For the further development of theoretical approaches of the regularities of plastic and postcritical deformation of fabrication materials and disruptive conditions, the critical task is to obtaining experimental data on the deformation regularity of materials under various types of stress-strain state under the conditions of strain localization in the neck form. To register inhomogeneous fields of displacements and strains in such tests, it seems appropriate to use optical methods of experimental mechanics, in particular, the modern perspective method of digital images correlation (DIC) [24].

The aim of the presented work is an experimental study of the mechanical behavior regularities of structural steels during postcritical deformation of specimens under the conditions of the strain localization formation in the neck form at tension.

MATERIALS AND EQUIPMENT

The specimens of structural steel 40Cr, the chemical composition of which is shown in Tab. 1, were used in the tests. The content of other elements, not listed in Tab. 1, is less than 0.025 % of each. Specimens for tests were made of a rod with a diameter of 16 mm, as-received state, without additional heat treatment.

Fe	C	Cr	Mn	Si	Cu	Ni	W
97.3 %	0.362 %	0.996 %	0.619 %	0.240 %	0.204 %	0.166 %	0.030 %

Table 1: Chemical composition of steel 40Cr.

Tensile tests at room temperature were carried out using the universal servohydraulic biaxial test system Instron 8850 (100 kN, 1000 N·m, 30 Hz) with the joint using of the noncontact 3D optical system for analyzing displacement and strain fields of Vic-3D Correlated Solutions based on the digital images correlation technique. Installation of the test equipment is shown in Fig. 1.

The samples were set in the V-shaped jaws of the hydraulic grips. The load in the tests was recorded by the Instron Dynacell load cell with an accuracy of no more than 0.4 % of the measured value. Extension of the specimens was recorded by the built-in displacement sensor of the test system. The stretching, deformation and diameter changing of the specimens in the test part were measured due to the video system data. The estimation of the accuracy of data recording by the video system was considered earlier in [24]. Data synchronization with the use of analog controller machine channels and video system were used during the testing. The registration of the displacement and strain fields was done with the high-resolution cameras Prosilica, with recorded frequency of 2 Hz, with set resolution of 16.0 MP with using of specialized illumination system. The relatively low frame rate is chosen, because of the monotony study process. Features description of the mathematical aspects of the video system, based on digital image correlation technique, as well as methodological aspects of the system application for solving problems related to solid mechanics is given in the following works [25, 26].

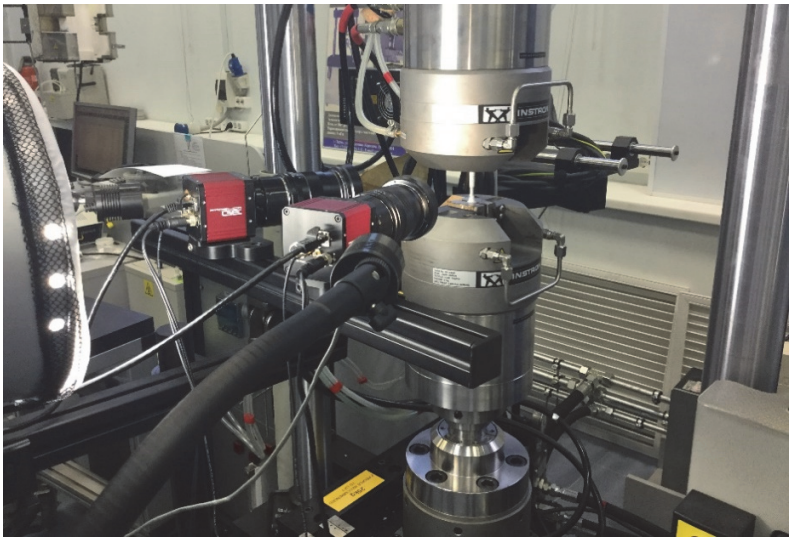

Figure 1: Installation of equipment for carrying out tension tests under combined using of biaxial test system Instron 8850 and 3D digital video system for analyzing of displacement and strain fields Vic-3D Correlated Solutions

TEST RESULTS

The approach used in the work is called "specimen from specimen", described earlier in [1, 7, 27]. For tensile tests, standard solid cylindrical specimens with a nominal diameter of the test part of 8 mm and with a length of 40 mm ($l_0 / d_0 = 5$) were made. The specimens were stretched to achieve different strain levels at the postcritical deformation stage, which was followed by necking effect. After achieving necessary levels of deformation, the samples were unloaded. There were done three different levels of deformation, achieved to the beginning of unloading, which parameters are presented in the Tab. 2, which contains the strain values ε, stresses σ and corresponding values of the coefficient of realization of the postcritical deformation stage $k_P = 1 - P_P / P_B = 1 - \sigma_P / \sigma_B$, possessing the following values of $0 \le k_P \le 1$.

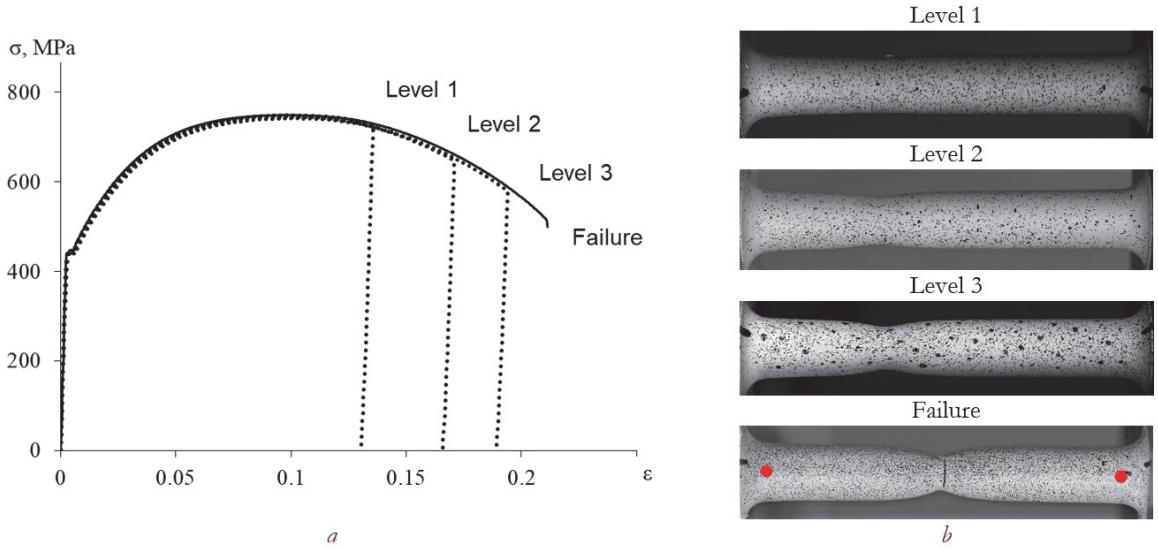

Figure 2: Strain curves (*a*) of steel 40Cr under tension up to failure (solid line) and tension curves up to various levels of postcritical deformation and unloadings (dashed lines); pictures of the test part of specimens with neck at different levels (*b*).

The value $k_P = 0$ is characterized by the absence of a postcritical deformation stage of material and corresponds to the failure when the tensile strength σ_B is achieved. And $k_P = 1$ is reached, that corresponds to the full implementation of the postcritical stage of deformation and is amounted to decreasing stresses (load) up to zero value by the moment of failure. Diagrams of stretching and unloading of the initial specimens of steel 40Cr in the coordinates "engineering stress - engineering strain" are given in Fig. 2 (*a*). Fig. 2 (*b*) shows pictures of the configuration of the gauge length of the specimens corresponding to the different levels of postcritical deformation and after failure, the red dots correspond to the marks between which the longitudinal displacements and deformations were recorded during the construction of the strain curves.

	ε, mm/mm	σ_P, MPa	k_P
Level 1	0.136	730	0.04
Level 2	0.171	650	0.15
Level 3	0.194	580	0.24

Table 2: Characteristic of levels of postcritical deformation achieved at the beginning of unloading.

According to the test procedure, the samples with the neck were turned in the test part to a diameter of 5.5 mm, which corresponded to the minimum diameter in the neck of specimen after unloading. The groove of specimens allows us to escape from the geometric nonlinearity of the test part, caused by the strain localization in the neck form. The turning of the specimens was carried out according to the two schemes, the sketches of the samples for which are shown in Fig. 3.

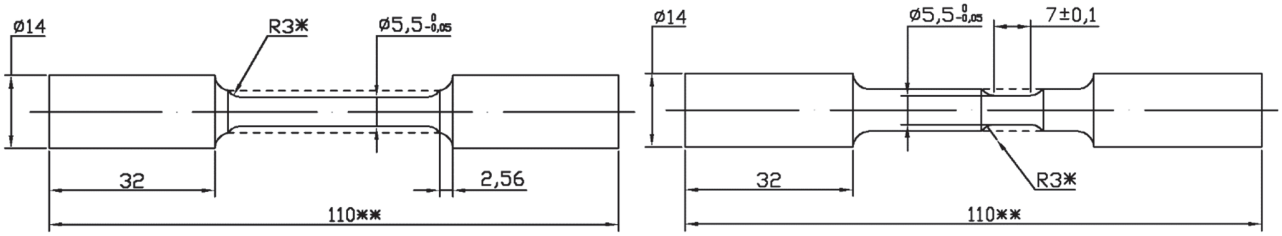

Figure 3: Turning schemes of test parts of specimens with neck (dashed lines corresponding to the geometry of initial specimen): *a* – scheme 1, *b* – scheme 2

The specimens made according to scheme 1 were used for estimate the evolution of the material mechanical properties in the gauge length of the specimen after necking, and the specimens, prepared according to scheme 2 were used for estimate the mechanical properties of steel directly in the neck zone. Fig. 4 shows the order of specimens processing and testing according to scheme 1 (*a-d*) and 2 (*e-h*).

In Fig. 4 (*a, e*) show the initial specimens before testing, after painting for recording by video system the frames for calculating the displacement fields. The pictures *b* and *f* in Fig. 4 are correspond to the specimens with strain localization in a neck-form after unloading at the postcritical deformation stage. The picture *c* in Fig. 4 shows the specimen which is after turning along the entire length of test part according to the sketch *a* in the Fig. 3, for further testing according to the scheme 1. Picture *g* in Fig. 4 presents a sample after turning in the area of the initial neck according to the sketch *b* in Fig. 3, for further testing according to scheme 2. Pictures *d* and *h* in Fig. 4 show the configurations of the destroyed specimens with newly formed strain localization in the neck-form after the tests according to the schemes 1 and 2, respectively.

Destruction of all samples made according to scheme 1 occurred in the peripheral part with respect to the necking zone at the initial specimens, as seen in Fig. 4 *(b* and *d)*. Strain curves obtained for specimens, which made according to scheme 1 and scheme 2, constructed by video system data, are shown in Fig. 5 (*a*) and (*b*), respectively: after unloading from the level 1 (solid line), after unloading from level 2 (dotted line) and after unloading from level 3 (dashed line).

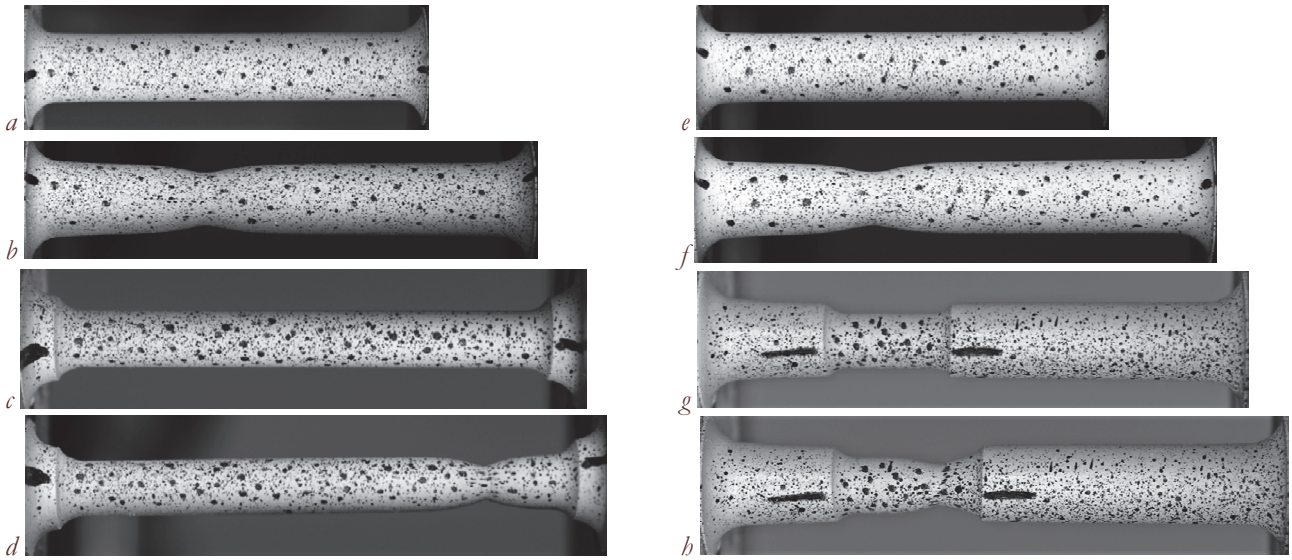

Figure 4: The order of turning and testing of specimens in accordance with scheme 1 (*a-d*) and scheme 2 (*e-h*).

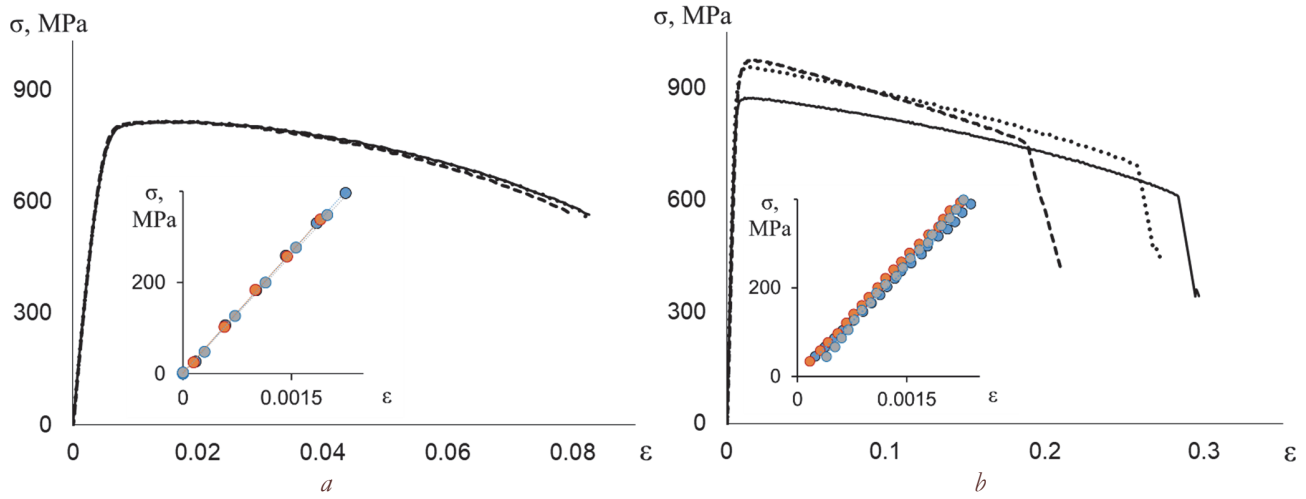

Figure 5: Strain curves obtained in the tests of specimens turned by scheme 1 (*a*) and scheme 2 (*b*) after tension of initial specimens at level a (solid lines), at level 2 (dotted lines) and level 3 (dashed lines), and initial stages of strain curves in the range of zero to 400 MPa.

Based on the obtained data, the values of the elasticity modulus at the initial linear sections of the strain curves were calculated in the stress range up to 400 MPa, which are shown on an enlarged scale in Fig. 5. The dependence of the values of the elastic modules of the tentative reached level of postcritical deformation and the scheme of specimens turning to the results of the tests was not revealed, which can be associated with a relatively small range of previously achieved deformations. The average value of the Young's modulus determined on the initial specimens was 204 GPa, and the average value after turning was 174 GPa. The deviation of experimental data obtained on the initial specimens by did not more than 5 %, and for all the turned specimens did not exceed 8 %. According to the test results, the maximum achieved stresses were calculated by the ratio of the maximum load to the initial cross-sectional area of the grooved specimens. The results reflecting the dependence of the ultimate stress upon stretching of samples turned along the entire gauge length (*a*) and turned in the necking zone (*b*) versus the degree of postcritical deformation reached at the moment of unloading, are shown in Fig. 6.

The obtained results may indicate that, at the time of unloading, the material in the peripheral zones of the initial specimens was in a hardened state, since the maximum stresses averaged by 10 % higher than the tensile strength of the initial specimens. In this case, the maximum stresses obtained by stretching the specimens prepared according to scheme 2 rise

with the increase in the previously achieved degree of postcritical deformation, which can be considered as an increase of the strength of steel in the necking zone with an increase by the previous deformation.

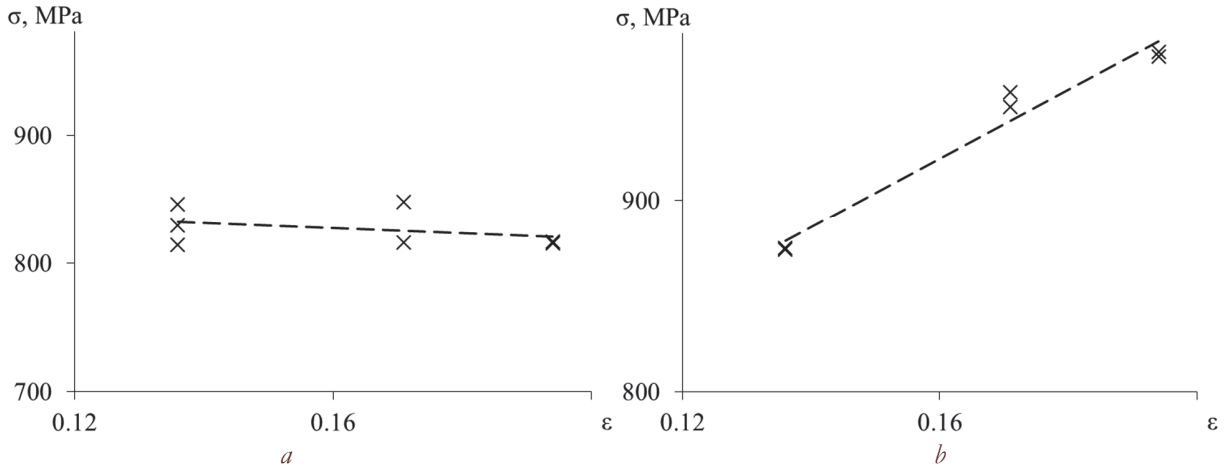

Figure 6: The ultimate stress obtained in tension tests of specimens turned along the entire length of test part (*a*) and specimens turned in the necking area (b) depending to level of the postcritical deformation achieved at beginning of unloading

In the Fig. 7 the extension curves of the initial specimens up to failure (solid line) and unloaded after reaching various levels of postcritical deformation (dotted lines) are shown. Strain curve of steel reflecting the change in the true stresses versus engineering strain (dashed line) obtained by the ratio of the load on the specimen to the current cross-sectional area of the specimen (by the minimum diameter), also is presented in the Fig. 7. The changing diameter of the test part $\angle d$ of the sample during the stretching was carried out using a three-dimension video system, by measurement of displacements along coordinate z, which coincide with radial direction of specimen. From the given data, it can be seen that the strain curve of true stresses has an increasing type at the postcritical deformation stage, which correlates with the calculated values of the critical stresses obtained by stretching the specimens done according to the scheme 2.

Fig. 8 shows the experimental data reflecting the distribution of longitudinal strains ε_{yy}, constructed at regular time intervals, along the length both initial samples (*a* and *b*), and for cases of specimens grooving along the entire length (*c*) and in the necking area (*d*).

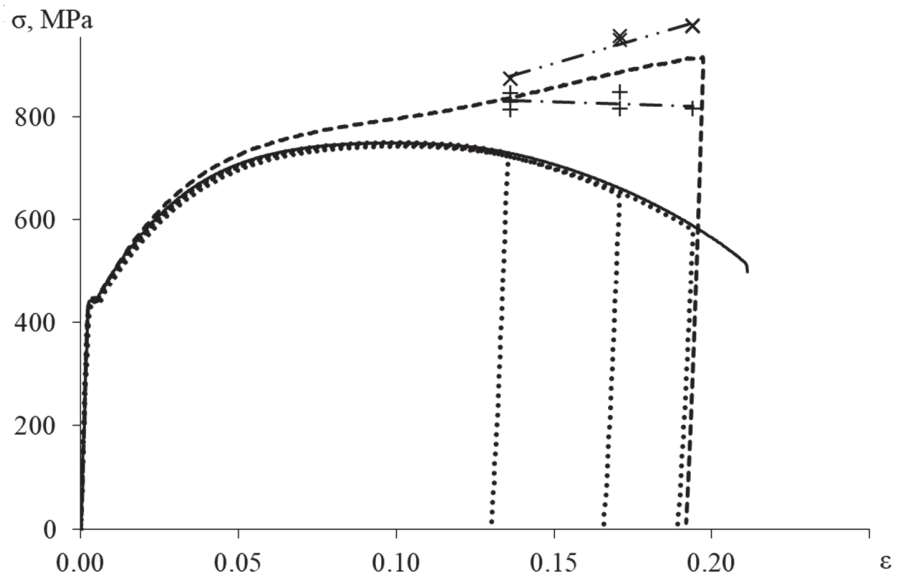

Figure 7: Strain curves of initial specimens at failure (solid line), after unloading at different levels of the postcritical deformation (dotted lines), strain curve obtained with account of the current cross-section area (dashed line); changing of ultimate stress obtained in tests by scheme 1 and 2 and correspondence trend lines (dash-dotted lines).

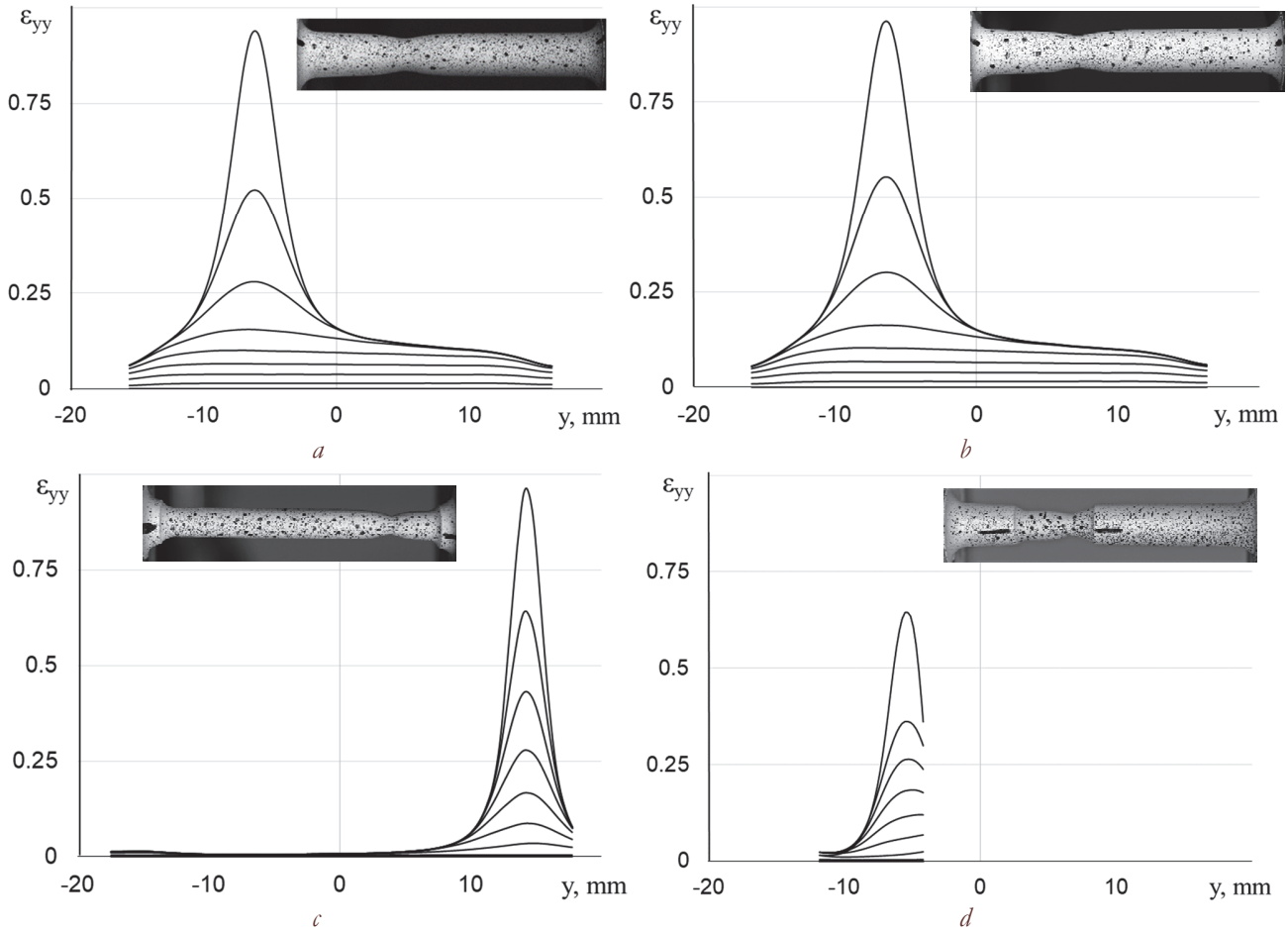

Figure 8: Distribution of longitudinal strain ε_{yy} along the length of test part of specimens at regular time intervals: initial specimens deformed to level 3 (*a* and *b*), specimen turned along entire length (*c*), specimen turned in necking area (*d*).

As you can see in the Fig. 8 (*a* and *b*), during tension of the initial specimens the longitudinal strain distribution is homogeneous along the length up to the 4-th profile, starting from the 5-th profile, strain localization and further neck formation are observed. Because of the analysis of the strain distribution in the tensile tests of specimens prepared according to the scheme 1 (Fig. 8, *c*), it was noted that the inhomogeneity of the longitudinal strain distribution is already observed from the 2-nd profile. The minimal longitudinal strain registered in the test part is corresponded to the necking zone on the initial specimen. Thus, in the case of tension the specimens turned along the entire length of test part, already at the initial stage of the test, strain is localized in the peripheral area of the test part of the initial specimen. The maximum longitudinal strain in the neck are comparable with the values of the maximum strain registered during the tension of the initial specimens, which indicates the presence of deformation reserves of the material in the peripheral area. At the same time, a lower level of maximum longitudinal strain in the neck of the specimens prepared according to scheme 2 (Fig. 8, *d*) demonstrates a decrease in the deformation reserves of the material in the neck zone of the initial specimen.

Conclusion

During the research work, an experimental study of the regularities of mechanical behavior of structural steel 40Cr under postcritical deformation of solid cylindrical specimens at tension was conducted. Particular attention is paid to the registration and interpretation of experimental data in the context of the formation of the strain localization as a necking effect. The results of the "specimen from specimen" test scheme are given. With preliminary stretching of the initial specimens, different levels of postcritical deformation are implemented. From the obtained specimens, the specimens

by two schemes were made to evaluate the material behavior in the absence of geometrical nonlinearity determined by the presence of a neck (a turning along the entire length) and to evaluate the state of the material directly in the necking zone. By using the noncontact 3D video system for recording the displacement and strain fields of Vic 3D Correlated Solutions based on the digital images correlation technique, registration of the displacement and strain fields in the gauge length of both the original specimens with the neck and after the groove ones according to the two different schemes was performed. According to the experimental results, the stiffness and strength of structural steel 40Cr were evaluated in a necked specimen at various stages of postcritical deformation. It is noted that the value of the modulus of elasticity does not depend significantly on the level of the previously achieved postcritical deformation and the way in which specimens are grooved. It is also shown that the material in the peripheral areas of the test part of the specimen can be in a strengthened state, which does not change at different degrees of previously achieved postcritical deformation. The strength of the steel 40Cr in the neck formation area is thereby increased and reaches values that can be 30 % higher the strength limit obtained during the stretching the initial specimens.

ACKNOWLEDGMENTS

The work is carrying out in Perm National Research Polytechnic University with financial support of grant of President of Russian Federation for government support of young Russian scientists (Grant № MK-3293.2017.1.) and with partial financial support of Russian Foundation for Basic Research (Grants № 17-48-590096 and № 17-48-590158).

REFERENCES

[1] Fridman, Y.B., Mechanical Properties of Metals, Moscow, Oborongiz, (1952).
[2] Vildeman, V.E., Sokolkin, Yu.V., Tashkinov, A.A., Mechanics of inelastic deformation and fracture of composite materials, Moscow, Nauka (1997).
[3] Bazant, Z.P., Di Luizo, G., Nonlocal microplane model with strain-softening yield limits, Intern. J. of Solids and Struct, 41 (2004) 7209–7240. DOI: 10.1016/j.ijsolstr.2004.05.065.
[4] Vildeman, V.E., Mechanics of postcritical deformation and questions of strength analysis methodology, International Journal for Computational Civil and Structural Engineering, 4 (2) (2008) 43.
[5] Struganov, V.V., Deformation stability of plastic beam under pure bending, Physical Mesomechanics, 7(S1-1) (2004) 169.
[6] Radchenko, V.P., Gorbunov, S.V., The method of solution of the elastic-plastic boundary value problem of tension of strip with stress raisers with allowance for local domains of softening plasticity of material, J. Samara State Tech. Univ., Ser. Phys. & Math. Sci., 4 (37) (2014) 98–110. DOI: 10.14498/vsgtu1366.
[7] Davidenkov, N.N., Spiridonova, N.I., Analysis of stress state in the neck of specimen under tension, Industrial laboratory (1945) 583-593.
[8] Ahmetzyanov, M.H., Albaut, G.N., Barishnikov, V.N., Investigation of stress-stain state in the neck of plate specimens of steels under tension by the method of photo-elastic coatings, Industrial laboratory. Materials diagnostics, 70(8) (2004) 41–51.
[9] Kukudzhanov, V.N., Levitin, A.L., Rheological instability and localization of strains in plane elastoplastic specimens under extension, Mechanics of Solids, 40 (6) (2005) 69-80.
[10] Bazhenov, V.G., Zhegalov, D.V., Pavlenkova, E.V., Numerical and experimental study of elastoplastic tension-torsion processes in axisymmetric bodies under large deformations, Mechanics of Solids 46(2) (2011) 204-212. DOI: 10.3103/S0025654411020087.
[11] Bai, Y., Teng, X., On the application of stress triaxiality formula for plane strain fracture testing, Journal of Engineering Materials and Technology, 131 (2009). DOI: 10.1115/1.3078390.
[12] Xue, Z., Pontin, M.G., Zok, F.W., Hutchinson, J.W., Calibration procedures for a computational model of ductile fracture, Engineering Fracture Mechanics, 77(3) (2010) 492-509. DOI: 10.1016/j.engfracmech.2009.10.007.
[13] Aretz, H., Keller, S., Vogt, R., Engler. O., Modelling of ductile failure in aluminum sheet forming simulation, Int J Mater Form 4 (2011) 163–182.

[14] Chu, X., Leotoing, L., Guines, D., Ragneau, E., Temperature and strain rate influence on AA5086 Forming Limit Curves: experimental results and discussion on the validity of the M-K model, International Journal of Mechanical Sciences, 78 (2014) 27-34. DOI: 10.1016/j.ijmecsci.2013.11.002.
[15] Wildemann, V.E., On the solutions of elastic-plastic problems with contact-type boundary conditions for solids with loss-of-strength zones, J. Appl. Maths Mechs, 62(2) (1998) 281.
[16] Faleskog, J., Barsoum, I., Tension-torsion fracture experiments. Part I: Experiments and a procedure to evaluate the equivalent plastic strain, International Journal of Solids and Structures, 50(25–26) (2013) 4241–4257. DOI: 10.1016/j.ijsolstr.2013.08.029.
[17] Tretiakov, M.P., Vildeman, V.E., Tests in tension-torsion conditions with descending sections of strain curve construction, Fracture and Structural Integrity, 24 (2013) 96–101. DOI: 10.3221/IGF-ESIS.24.10.
[18] Tretyakov, M.P., Experimental investigation of the postcritical deformation stage of materials under tension and torsion, PhD thesis, Institute of Continuous Media Mechanics (2014).
[19] Tretyakov, M.P., Wildemann, V.E., Lomakin, E.V., Failure of materials on the postcritical deformation stage at different types of the stress-strain state, Procedia Structural Integrity, 2 (2016) 3721-3726. DOI: 10.1016/j.prostr.2016.06.462.
[20] Wildemann, V.E., Lomakin, E.V., Tretyakov M.P., Postcritical deformation of steels in plane stress state, Mechanics of Solids, 49(1) (2014) 18-26. DOI 10.3103/S0025654414010038.
[21] Sokolkin, Y.V., Vildeman, V.E., Zaitsev, A.V., Rochev, I.N., Structural damage accumulation and stable postcritical deformation of composite materials, Mechanics of Composite Materials, 34(2) (1998) 171.
[22] Ilinykh, A.V., Radionova, M.V., Vildeman, V.E., Computer synthesis and statistical analysis of the distribution of structural characteristics of granular composite materials, Composites: Mechanics, Computations, Applications, 2(2) (2011) 95.
[23] Wildemann, V.E., Ilyinykh, A.V., Simulation of structural failure and scale effects of softening at the post-critical deformation stage in heterogeneous media, Physical Mesomechanics, 10(4) (2007) 23.
[24] Tretyakova, T.V., Tretyakov, M.P., Wildemann, V.E. Estimate of measurements accuracy by using video-system of displacement and strain fields analysis, PNRPU Mechanics Bulletin, 2 (2011) 92-100.
[25] Tretyakova, T.V., Wildemann, V.E., Spatial-time inhomogeneity of the processes of inelastic deformation of metals, Moscow, Fizmatlit, (2016).
[26] Tetyakova, T.V., Wildemann, V.E., Influence the loading conditions and the stress concentrators on the spatial-time inhomogeneity due to the yield delay and the jerky flow: study by using the digital image correlation and the infrared analysis, Frattura ed Integrità Strutturale, 42 (2017) 303-314; DOI: 10.3221/IGF-ESIS.42.32
[27] Vildeman, V.E., Lomakin, E.V., Tret'yakova, T.V., Tret'yakov, M.P. Development of inhomogeneous fields under postcritical deformation of steel specimens in extension, Mechanics of Solids, 51(5) (2016) 612-618. DOI: 10.3103/S0025654416050150.

NOMENCLATURE

l_0	initial length of specimen test part
d_0	initial diameter of specimen test part
$\triangle d$	changing of diameter of specimen test part at tension
σ	engineering stress
σ_B	ultimate stress
σ_P	the stress corresponding to the failure (or beginning of the unloading) at the postcritical deformation stage
P_B	the load corresponding to the ultimate stress (or maximum load)
P_P	the load corresponding to the failure (or beginning of the unloading) at the postcritical deformation stage
ε	longitudinal strain by DIC system
ε_{yy}	strain along the coordinate y by DIC system
y	coordinate corresponding to the longitudinal axis of specimen
z	coordinate corresponding to the radial axis of specimen
$k_{\varepsilon P}$	coefficient of the postcritical deformation stage realization